# Analytical Modeling and Torque Ripple Reduction for Permanent Magnet Synchronous Motor with Stator Winding Unbalance Fault

Ahmed Belkhadir, Driss Belkhayat, Youssef Zidani, Remus Pusca, Raphael Romary, Oussama-Ali Dabaj

# Analytical Modeling and Torque Ripple Reduction for Permanent Magnet Synchronous Motor with Stator Winding Unbalance Fault

Ahmed Belkhadir[1*], Driss Belkhayat[1], Youssef Zidani[1], Remus Pusca[2], Raphaël Romary[2], Oussama-Ali Dabaj[1]

[1] Faculty of Sciences and Technologies, Cadi Ayyad University, Electrical Systems, Energy Efficiency and Telecommunications laboratory (LSEEET), Marrakesh, Morocco.

[2]Laboratory of Electrical Systems and Environment (LSEE), Artois University, Béthune, France

ahmed.belkhadir@ced.uca.ma, driss.belkhayat@uca.ma, y.zidani@uca.ma, remus.pusca@univ-artois.fr, raphael.romary@univ-artois.fr, oussama-ali.dabaj@ced.uca.ma

**Abstract**

The presence of a fault in electrical machines is able to generate disturbances in its operation. It can be noise, vibrations or torque ripples. This paper proposes a technique and control method allowing to reduce torque ripples and consequently vibrations. The fault generates considerable constraints, and disturb operation leading to decrease performances. In our study, the fault considered concerns unbalanced stator winding applied to a permanent magnet synchronous motor (PMSM) illustrated by a lack of turns in one of its windings. The proposed approach is based on the space phasor of currents and fluxes in order to calculate the reference currents by vector method allowing to correct the fault. A theoretical concept is presented to validate the implementation of the fault control principle. The studied structure has been verified using MATLAB/Simulink under several values parameters.

**Keywords—** Reduction of torque ripples, permanent magnet synchronous motor, lack of turns winding, space phasor, vectorial approach.

## 1 Introduction

Due to their performances, PMSM are widely used in a several applications such as aerospace, electric vehicles, industry and robotics... [1]. As shown in Figure 1, the PMSM has the highest energy density and overall efficiency (the green color) [2], but on the other hand the induction machine has a higher reliability, robustness and a lower cost compared to the PMSM [3], which makes it an excellent choice for applications used in electric mobility.

However, the torque ripples generated by PMSM lead to negative effects on the operation regime such as noise, vibration and reduced motor efficiency [4].

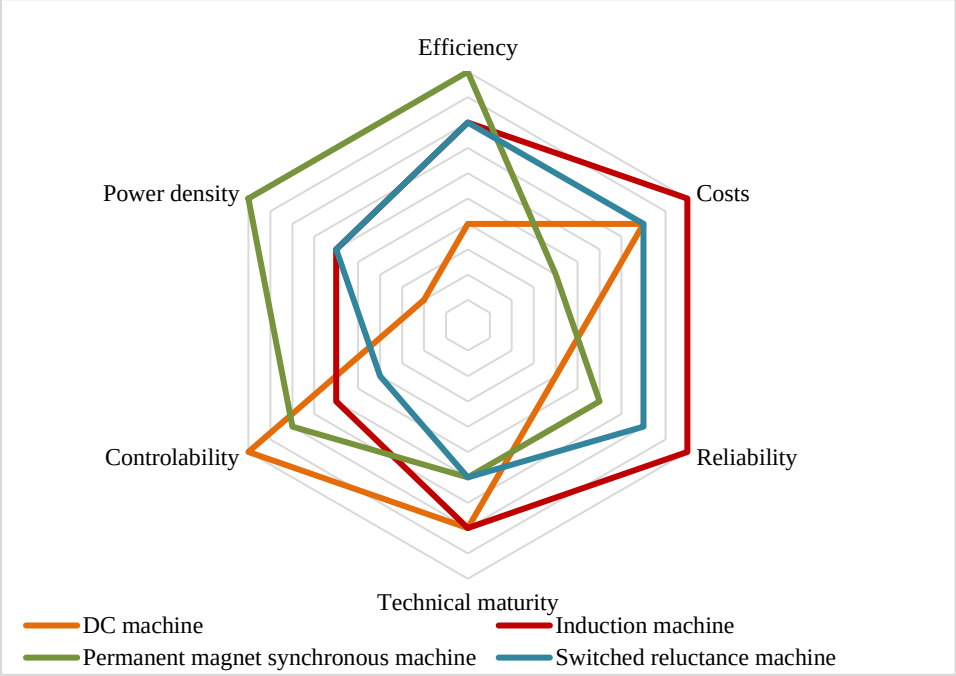


**Figure 1:** Evaluation of the electrical machines

Torque ripples in electrical machines occur for many reasons and faults, for example: non-sinusoidal supply voltage, asymmetry in design [5], lack of stator windings, short-circuit between turns, rotor eccentricity or a magnetic circuit fault [6] – [7]. Monitoring and diagnosis of these machines is an essential part of reliability and dependability in order to ensure continuity of service.

In recent years, extensive studies and research have been conducted on methods of controlling and reducing torque ripples. The most commonly used consists to reduce the ripples by injecting a harmonic current to the motor [4] – [8]. Other methods propose the generation of optimal reference currents for multiphase permanent magnet synchronous machines using a vector approach in order to maintain a constant torque [9].

Another strategy is to control the stator currents using a dual frame of reference in order to compensate for oscillations due to the current harmonic, so that the positive and negative sequence current and voltage components were controlled in their own frame of reference [10].

In this paper, a control method is proposed for the minimization of torque ripples in the case of an electrical fault. The following approach is based on electrical models using current and flux space phasors [11]. These quantities are measurable or estimable and can be controlled by the control technique. The space phasor is an interesting tool since it performs a two-axis transformation while allowing for easy reference frame changes [12]. However, the space phasor is based on fundamental assumptions. The electric motor will be considered in the healthy state, as well as the magnetomotive force has a sinusoidal spatial distribution.

The objective of the present work is to develop a control strategy in the case of a lack of turn on a stator phase.

Therefore, the paper is presented as follows: after the introduction section, a mathematical dynamic model of PMSM is described. The implementation of the control system is detailed. Then, the reduction of torque ripples is shown followed by tests and simulations results. And finally, conclusion.

# 2 Mathematical model of PMSM

The equivalent circuit diagram of the PMSM shown in Figure 2, which is used as a reference. By using the abc reference model, it is easy to introduce the lack of turns fault. The abc model is used to quantify the impact of the fault and to take into account the unbalance of the stator winding in the control technique in order to limit the torque ripples.

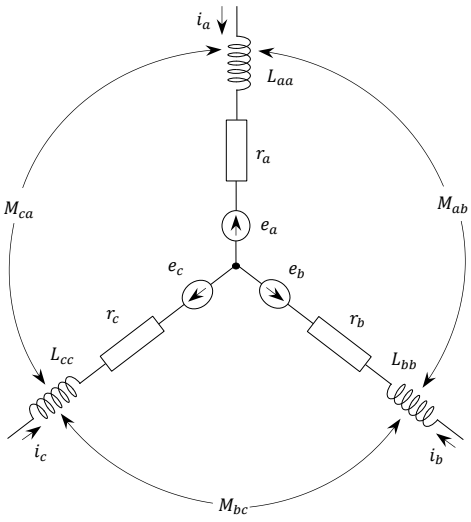


**Figure 2:** Circuit diagram of the PMSM

## 2.1 Healthy PMSM in the abc frame

The electrical equations in the abc reference frame are as follows:

$$[V_{s,abc}] = [r_{s,abc}].[i_{s,abc}] + \frac{d}{dt}[\phi_{s,abc}] \quad (1)$$

Where the phase voltages and currents can be expressed as:

$$[V_{s,abc}] = [V_a \quad V_b \quad V_c]^T \qquad \text{and} \qquad [i_{s,abc}] = [i_a \quad i_b \quad i_c]^T$$

The stator magnetic flux is composed of the flux linkage due to stator windings plus the one due to rotor permanent magnets as expressed in:

$$[\phi_{s,abc}] = [L_{abc}].[i_{s,abc}] + [\phi_{r,abc}] \quad (2)$$

Where $[r_{s,abc}] = \begin{bmatrix} r_a & 0 & 0 \\ 0 & r_b & 0 \\ 0 & 0 & r_c \end{bmatrix}$, $[L_{abc}] = \begin{bmatrix} L_{aa} & M_{ab} & M_{ac} \\ M_{ba} & L_{bb} & M_{bc} \\ M_{ca} & M_{cb} & L_{cc} \end{bmatrix}$ and $[\phi_{s,abc}] = [\phi_a \quad \phi_b \quad \phi_c]^T$

The rotor flux expressed in the abc reference frame due to the rotor:

$$[\phi_{r,abc}] = \phi_{PM}.\left[\cos(\theta) \quad \cos(\theta - \frac{2\pi}{3}) \quad \cos(\theta + \frac{2\pi}{3})\right]^T \tag{3}$$

Where $[\phi_{r,abc}] = [\phi_{ra} \quad \phi_{rb} \quad \phi_{rc}]^T$ and $\theta = p.\theta_m$

From (1) and (2), it results in the general equation:

$$[V_{s,abc}] = [r_{s,abc}].[i_{s,abc}] + [L_{abc}].\frac{d}{dt}[i_{s,abc}] + \frac{d}{dt}[\phi_{r,abc}] \tag{4}$$

The sum of the stator currents is equal to zero:

$$i_a + i_b + i_c = 0 \tag{5}$$

The stator magnetic fluxes are defined as:

$$\begin{bmatrix}\phi_a\\ \phi_b\\ \phi_c\end{bmatrix} = \begin{cases}\phi_a = L_{aa}.i_a + M_{ab}.i_b + M_{ac}.i_c + \phi_{ra}\\ \phi_b = M_{ba}.i_a + L_{bb}.i_b + M_{bc}.i_c + \phi_{rb}\\ \phi_c = M_{ca}.i_a + M_{cb}.i_b + L_{cc}.i_c + \phi_{rc}\end{cases} \tag{6}$$

The stator flux is expressed with only ia and ib currents, we obtain the following equations:

$$\begin{bmatrix}\phi_a\\ \phi_b\\ \phi_c\end{bmatrix} = \begin{bmatrix}L_{aa} - M_{ac}\\ M_{ba} - M_{bc}\\ M_{ca} - L_{cc}\end{bmatrix}.[i_a] + \begin{bmatrix}M_{ab} - M_{ac}\\ L_{bb} - M_{bc}\\ M_{cb} - L_{cc}\end{bmatrix}.[i_b] + \begin{bmatrix}\phi_{ra}\\ \phi_{rb}\\ \phi_{rc}\end{bmatrix} \tag{7}$$

The potential of the neutral point can vary in the presence of the fault. Therefore, we use the voltage equations without the introduction of $V_n$.

The voltage and current equations can be reduced to five independent equations of $V_n$:

$$\begin{cases}\frac{d}{dt}\phi_a - \frac{d}{dt}\phi_b = V_a - V_b - r_a.i_a + r_b.i_b\\ \frac{d}{dt}\phi_b - \frac{d}{dt}\phi_c = V_a - V_c - (r_a + r_c).i_a + r_c.i_b\end{cases} \tag{8}$$

$$i_a = \frac{(\phi_a - \phi_{ra} - \phi_b + \phi_{rb}) - (M_{ab} - M_{ac} - L_{bb} + M_{bc}).i_b}{L_{aa} - M_{ac} - M_{ba} + M_{bc}} \tag{9}$$

$$i_b = \frac{(\phi_a - \phi_{ra} - \phi_c + \phi_{rc}) - (L_{aa} - M_{ac} - M_{ca} + L_{cc}).i_a}{M_{ab} - M_{ac} - M_{cb} + L_{cc}} \tag{10}$$

$$i_c = -(i_a + i_b) \tag{11}$$

## 2.2 The electromagnetic torque

The expression of the electromagnetic torque is obtained from the vector product between the space phasor of the flux and the current:

$$\Gamma_e = \frac{3}{2}.p.(\overline{\phi_s} \wedge \overline{i_s}) \tag{12}$$

The space phasor of the current and the flux are as follows:

$$\overline{i_s} = \frac{2}{3}(i_a + i_b.a + i_c.a^2) \tag{13}$$

$$\overline{\phi_s} = \frac{2}{3}(\phi_a + \phi_b.a + \phi_c.a^2) \tag{14}$$

Where: $a = e^{j(\frac{2\pi}{3})} = -\frac{1}{2} + j\frac{\sqrt{3}}{2}$

Considering the real and imaginary components of the space phasor of the current:

$$\begin{cases} i_d = \Re(\overline{i_s}) \\ i_q = \Im(\overline{i_s}) \end{cases} \tag{15}$$

Using $1 + a + a^2 = 0$, a new expression of the flux space vector will be used:

$$\overline{\phi_s} = -\frac{2}{3}[a.(\phi_a - \phi_b) + a^2.(\phi_a - \phi_c)] \tag{16}$$

## 2.3 the mechanical equation

The conversion of electrical energy into mechanical energy in rotating machines is determined by the following relation:

$$\Gamma_e - \Gamma_r - F\Omega = J\frac{d}{dt}\Omega \tag{17}$$

Where: $\theta = \int \Omega \, dt$

## 2.4 Model of the proposed structure

Proposed structure using the space phasor is described in the Figure 3. In this model, the flux is calculated from the voltage and currents. The electromagnetic torque is determined from the space phasor of the flux and the currents, the rotation angle is given by the mechanical equation. The currents supplying the PMSM are obtained from the electrical equations (9, 10 and 11).

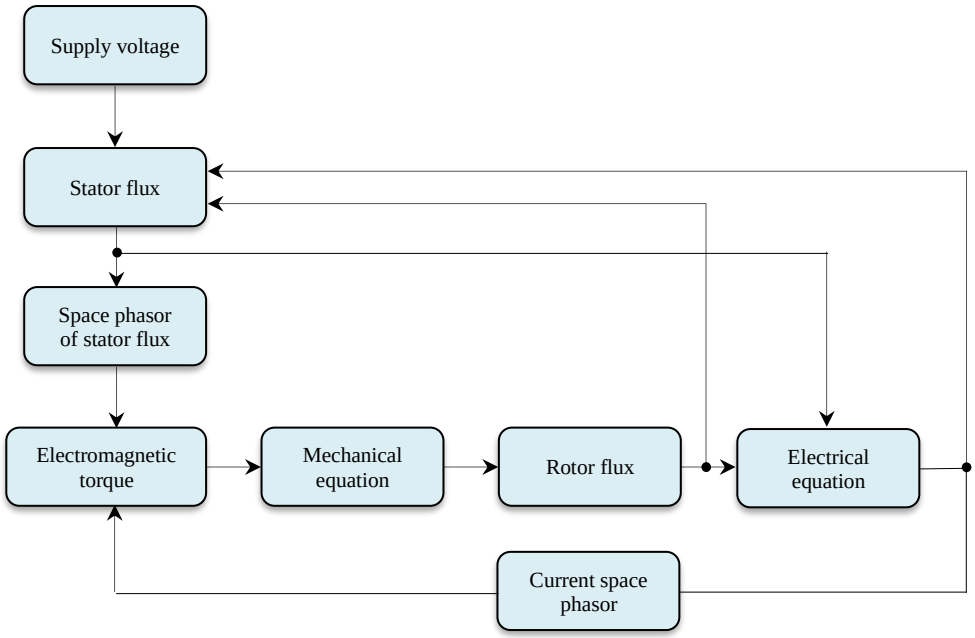


**Figure 3:** Block diagram of the model used in simulation

# 3 The implementation of the control system

The control strategy in the case of our study is to minimize the ripples with current control. According to the study of the torque equation (12) which is derived from a vector product between the flux and current space phasor. Therefore, to produce a maximum torque it is necessary that the current and the flux are in quadrature. Therefore, the control law must follow a torque that is constant and maximum, which means that the flux is in quadrature with the current.

$$\Gamma_e{}^* = \frac{3}{2}.p.\left(\phi_d.i_q{}^* - \phi_q.i_d{}^*\right) = cste \tag{18}$$

$$\phi_d.i_d{}^* = -\phi_q.i_q{}^* \tag{19}$$

$$i_d{}^* = -\frac{\phi_q.i_q{}^*}{\phi_d} \tag{20}$$

$$i_q{}^* = -\frac{\phi_d.i_d{}^*}{\phi_q} \tag{21}$$

By replacing equations (20) and (21) in equation (18), the reference currents giving a constant torque without ripples are obtained:

$$\begin{cases} i_d{}^* = -\dfrac{2}{3p}.\Gamma_e{}^*.\dfrac{\phi_q}{\phi_d{}^2+\phi_q{}^2} \\ i_q{}^* = \dfrac{2}{3p}.\Gamma_e{}^*.\dfrac{\phi_d}{\phi_d{}^2+\phi_q{}^2} \end{cases} \tag{22}$$

Considering the real and imaginary components of the space phasor of the flux:

$$\begin{cases} \phi_d = \Re(\overline{\phi_s}) \\ \phi_q = \Im(\overline{\phi_s}) \end{cases} \tag{23}$$

The space phasor of the reference current is expressed in terms of its real and imaginary parts:

$$\overline{i_s{}^*} = i_d{}^* + j.i_q{}^* \tag{24}$$

The reference currents are given by the following equations:

$$\begin{cases} i_a{}^* = \Re(\overline{i_s{}^*}) \\ i_b{}^* = \Re(a.\overline{i_s{}^*}) \\ i_c{}^* = \Re(a^2.\overline{i_s{}^*}) \end{cases} \tag{25}$$

To simulate the faulty case, we consider a simplified diagram of the stator winding to show the interaction between the stator phase windings in the case of a lack of turns presented on Figure 4. Each phase consists of six elementary sections. Each of these sections is decomposed into three equal parts, which allows the injection of the fault.

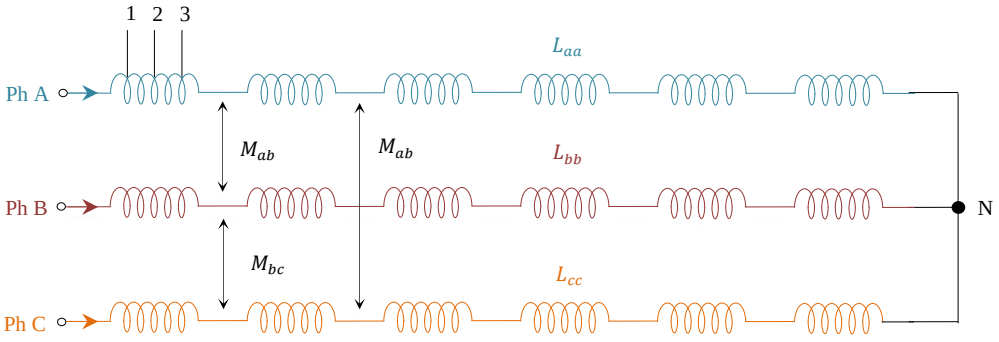


**Figure 4:** Structure of the stator winding of the machine

The tests corresponding to the machine for operation under load, considering two levels of severity of the fault:

- A lack of turns of 10% of the elementary section;
- A lack of turns of 25% of the elementary section.

To simulate the control system, the control loop shown in Figure 5 is used. It consists in calculating the reference currents from a reference torque delivered by the speed control loop and the space phasor of the flux estimated by integration of the supply voltages (equation (8)). The reference speed considered in the control is 1500 rpm which corresponds to a power supply frequency of 50 Hz.

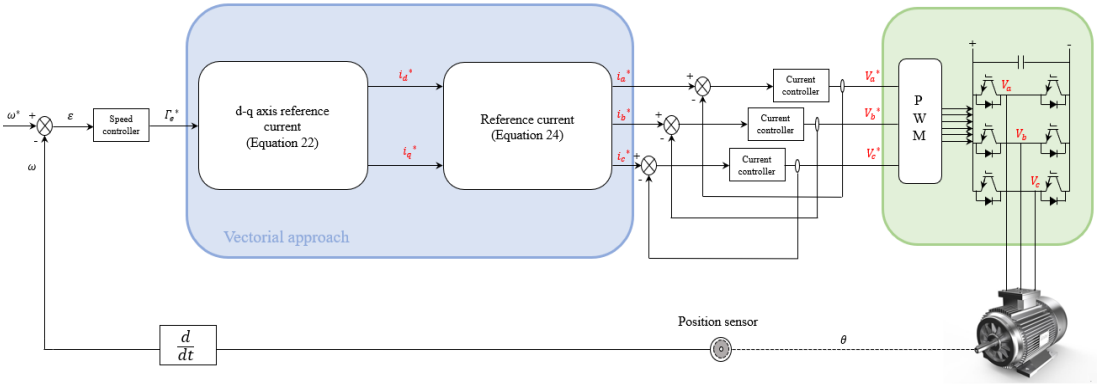


**Figure 5:** Diagram of the control loop with fault correction

# 4 Simulation results

## 4.1 Simulation results without fault correction

The Simulink model used to verify the structure of control loop is presented in Figure 6. The PMSM parameters values are shown in Table 1.

The proposed approach is verified using MATLAB/Simulink. The following simulations are carried for two levels of faults. The currents, the torque delivered by the PMSM and the speed will be measured to evaluate the performance of the control loop and quantify the ripples. Two cases of scenarios will be taken during the simulation: the PMSM is powered by a three-phase balanced current system in the first case. Secondly, the motor will be supplied by the currents id and iq (Equation 22) giving a constant torque without ripples. The fault is applied at 12 s. Figure 7 (a and b) shows the electromagnetic torque in case of a fault. at 12 s, the torque has ripples corresponding to the twice of the supply frequency.

This type of defect can be detected by experimental validation using sensors to analyze the magnetic field of dispersion [13] – [14]. From a diagnostic point of view, the advantage of this method is that it is non-invasive and simple to implement.

As shown in Figure 8 (a and b) which illustrates the speed in case of fault 1 and 2, we can see the speed variation between two maximum and minimum values. We also notice speed ripples at twice the supply frequency and an increase in these ripples (Figure 8a) compared to fault case 1 (Figure 8a).

Figure 9, Figure 10 and Figure 11 show respectively the currents absorbed by the motor, as well as the d-q axis currents of the stator in case of fault. We notice the increase of the maximum value of the absorbed current due to the fault compared to the healthy case.

## 4.2 Simulation results with fault correction

To verify the proposed structure, we adopt the model presented in Figure 5 and Figure 6.

Figure 13a shows an electromagnetic torque analysis that gives us low ripples using the control loop that is based on the space phasor approach. To analyze the evolution of the PMSM speed under fault

with the correction, Figure 13b is presented. It can be seen that the speed variation is much smaller than in the same case without correction. Also, we notice that we have good performance indices for the transient state such as the response time and rise time.

Figure 14a, Figure 14b and Figure 15a show respectively the stator currents absorbed by the motor and the d-q axis currents of the stator in the case of the fault correction. According to the simulation, we can see that the currents absorbed in the fault case follow the currents in the healthy case. This is due to the control generating an unbalanced three-phase current system to compensate for the unbalance introduced by the lack of windings fault.

Table 2 is a summary of the results obtained by the simulation. We notice that the level of the torque ripples depends on the level of the fault. Also, as the fault level increases, the speed, torque and current ripples increase. The correction leads to a reduction of these ripples.

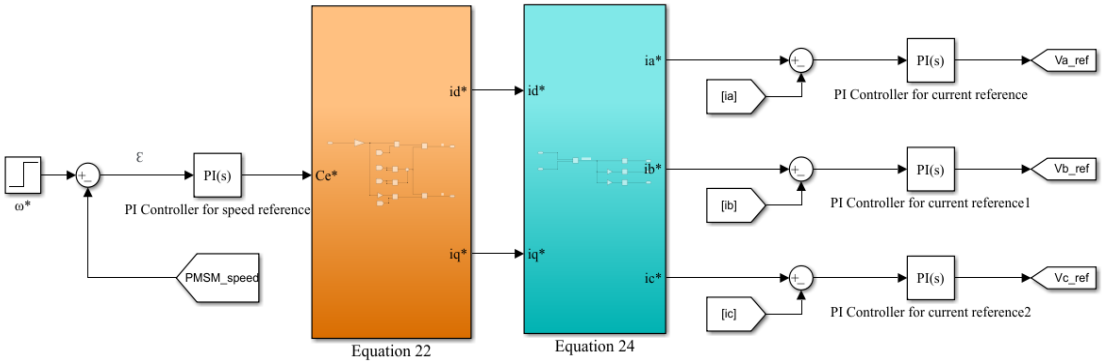


**Figure 6:** Simulink model of the control structure

| Parameters | | Units |
|---|---|---|
| $r_a, r_b, r_c$ | 2.5 | Ω |
| $L_{aa}, L_{bb}, L_{cc}$ | 82.4 | $mH$ |
| $M_{ab}, M_{bc}, M_{ac}$ | -41.2 | $mH$ |
| $J$ | 0.00248 | $Kg.m^2$ |
| $F$ | 18 | $Nm.s.rad^{-1}$ |
| $p$ | 2 | |

**Table 1:** PMSM parameters

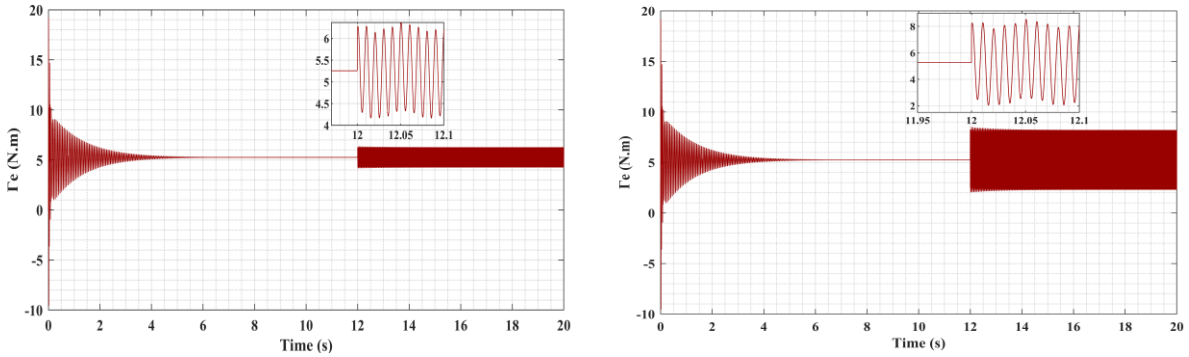


(a) (b)

**Figure 7:** Electromagnetic torque, ((a) Fault 1, (b) Fault 2)

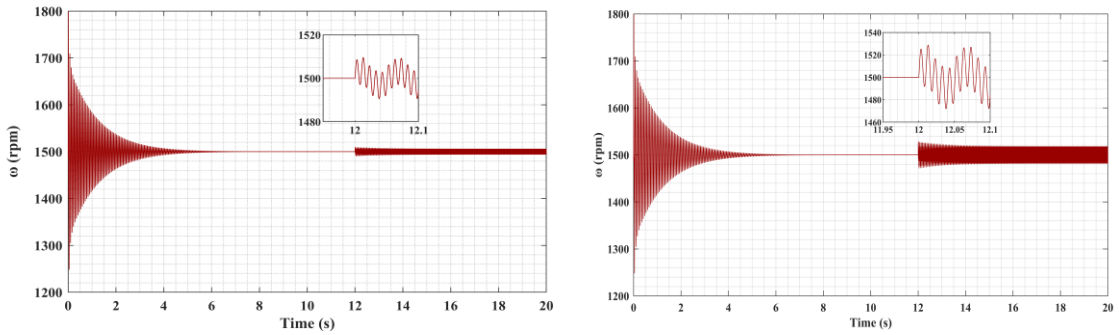


(a) (b)

**Figure 8:** Rotor speed, ((a) Fault 1, (b) Fault 2)

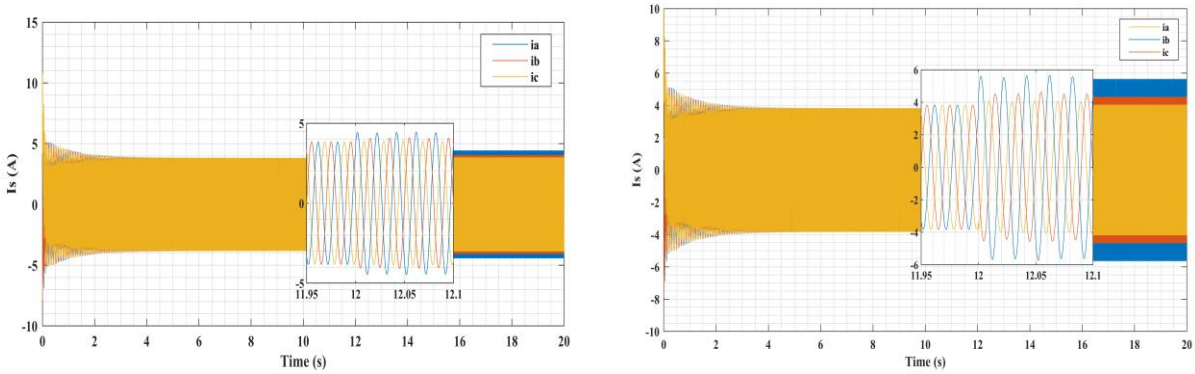


(a) (b)

**Figure 9:** Stator current, ((a) Fault 1, (b) Fault 2)

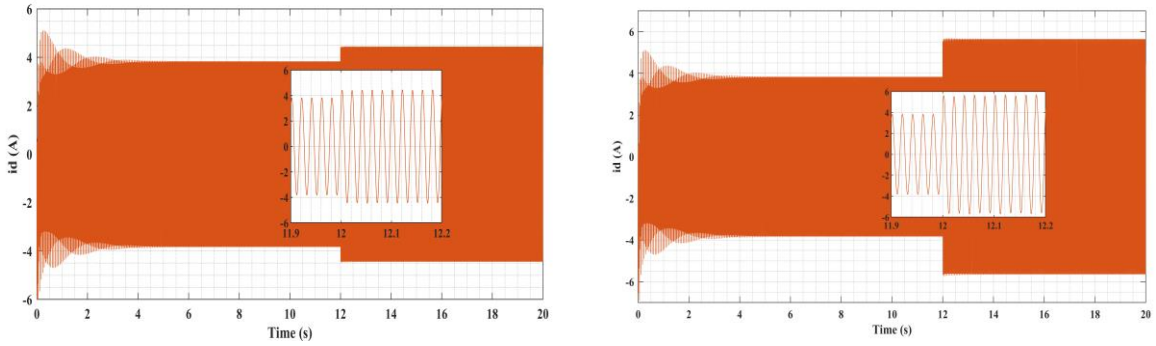


(a) (b)

**Figure 10:** d-axis stator current, ((a) Fault 1, (b) Fault 2)

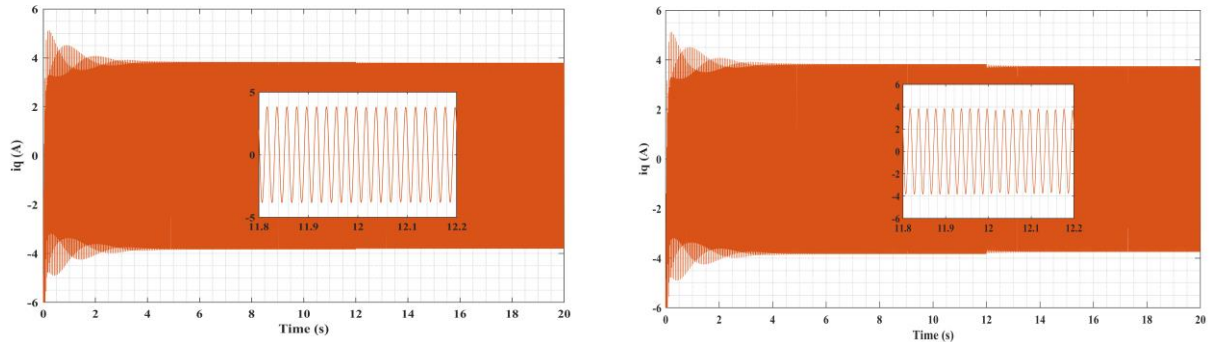


(a) (b)

**Figure 11:** q-axis stator current, ((a) Fault 1, (b) Fault 2)

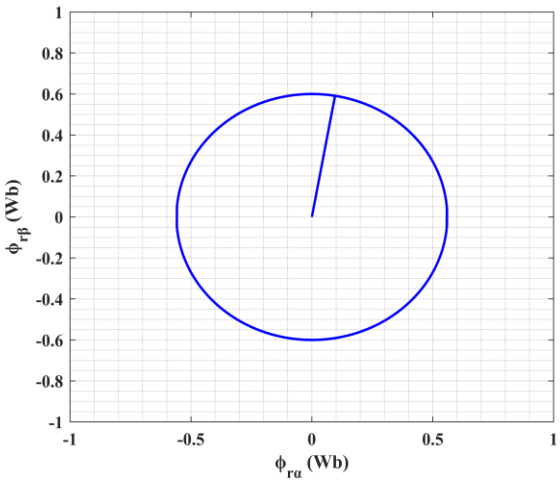


**Figure 12:** Trajectory of the rotor flux in the stationary frame

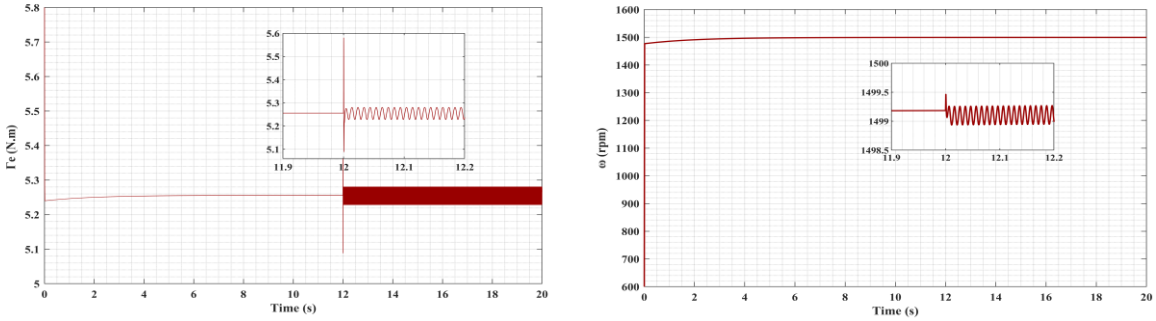


(a) (b)

**Figure 13:** (a) Electromagnetic torque, (b) Rotor speed

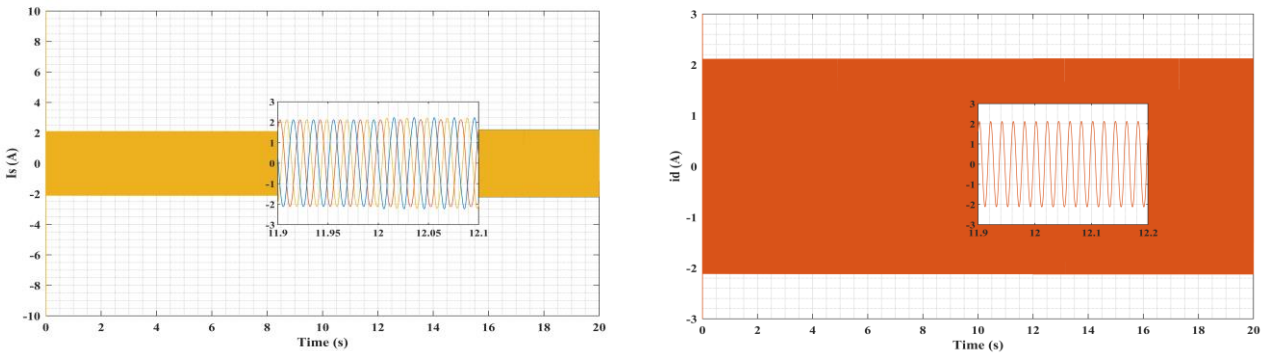


(a) (b)

**Figure 14:** (a) Stator current, (b) d-axis stator current

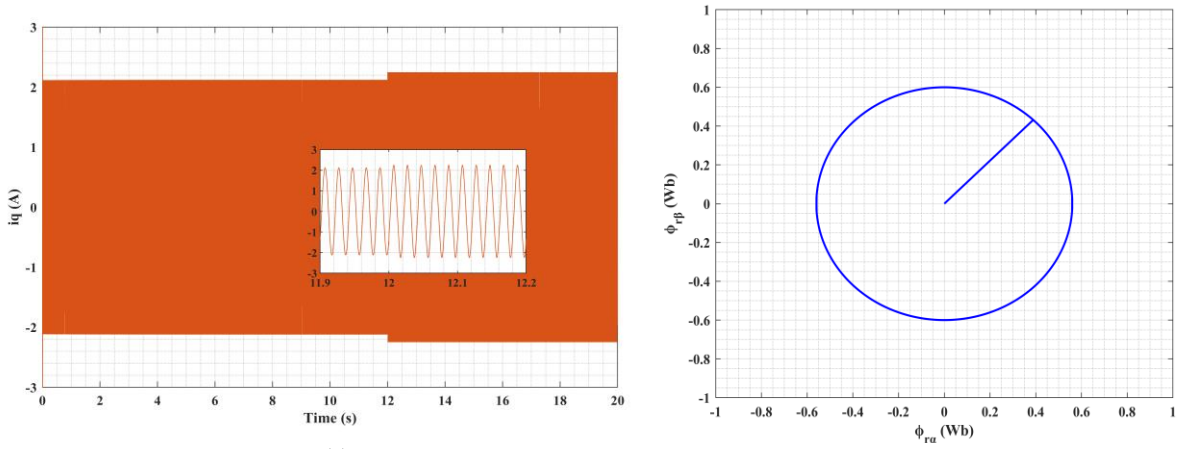


(a) (b)

**Figure 15:** (a) q-axis stator current, (b) Trajectory of the rotor flux in the stationary frame

| | Healthy | Fault 1 without correction | Fault 2 without correction | Fault 1 with correction | Fault 2 with correction |
|---|---|---|---|---|---|
| $\Gamma_e\ (N.m)$ | 5.26 | 6.37 | 8.53 | 5.28 | 5.31 |
| $i_{a,max}(A)$ | 3.83 | 4.45 | 5.57 | 2.23 | 2.42 |
| $i_{b,max}(A)$ | 3.83 | 3.87 | 4.04 | 2.16 | 2.34 |
| $i_{c,max}(A)$ | 3.83 | 4.04 | 4.47 | 2.21 | 2.13 |
| $i_{a,max}{}^{*}\ (A)$ | 1.97 | - | - | 2.003 | 2.006 |
| $i_{b,max}{}^{*}\ (A)$ | 1.97 | - | - | 2.09 | 2.28 |
| $i_{c,max}{}^{*}\ (A)$ | 1.97 | - | - | 2.06 | 2.22 |
| $\varepsilon_a$ | - | - | - | 0.26 | 0.28 |
| $\varepsilon_b$ | - | - | - | 0.25 | 0.27 |
| $\varepsilon_c$ | - | - | - | 0.23 | 0.2 |
| $\omega(rpm)$ | 1500.07 | 1509.64 | 1528.78 | 1499.27 | 1499.54 |
| $\varepsilon_\omega$ | - | - | - | 0.02 | 0.04 |

**Table 2:** Summary of the results obtained by the simulation in case of a lack of turns fault

# 5 Conclusion

In the present paper, an improved approach of torque ripple reduction for permanent magnet synchronous motor is presented. The results obtained for a healthy and defective case modeling for two different values of the lack of stator windings fault. The increase of torque ripples has been clearly shown in presence of the fault. The approach used to minimize these ripples was based on the space phasor by injecting an unbalanced three-phase system of currents to compensate the effects introduced by the fault. In order to validate this work, simulations are performed for different values of defects in the stator winding with an active control approach that allows to impose the right current references. The immediate perspectives are to implement and to use an adaptive control with intelligent algorithms to reduce the effects caused by faults in electrical machines.

# Nomenclature

| | |
|---|---|
| $[i_{s,abc}], [V_{s,abc}]$: | Stator three-phase current and voltage matrix |
| $[r_{s,abc}]$: | Stator resistance matrix |
| $[\phi_{s,abc}], [\phi_{r,abc}]$: | Stator and rotor flux matrix |
| $\phi_{PM}$: | Permanent magnet flux |
| $[L_{abc}]$: | Stator inductance matrix |
| $L_{aa}, L_{bb}, L_{cc}$: | Self-inductances of the stator windings |
| $M_{ab}, M_{ac}, M_{bc}$: | Mutual inductances of the stator windings |
| $\theta, \theta_m$: | Rotor electrical and mechanical position |
| $p$: | Number of pole pairs |
| $\Gamma_e, \Gamma_e{}^*, \Gamma_r$: | Electromagnetic, reference electromagnetic and load torques |
| $\overline{\phi_s}$: | Space phasor of stator flux |
| $\overline{i_s}$: | Space phasor of stator currents |
| $\overline{i_s{}^*}$: | Space phasor of reference current |
| $F$: | Friction coefficient |
| $J$: | Total inertia |
| $\Omega$: | Rotor angular speed |
| $\phi_d, \phi_q$: | d-q axis flux |
| $i_d{}^*, i_q{}^*$ : | d-q axis reference current |
| $i_a{}^*, i_b{}^*, i_c{}^*$: | abc frame reference current |
| $\Re(\overline{\phi_s}), \Re(\overline{i_s}), \Re(\overline{i_s{}^*})$: | Real part of $(\overline{\phi_s}, \overline{i_s}, \overline{i_s{}^*})$ |
| $\Im(\overline{\phi_s}), \Im(\overline{i_s})$: | Imaginary part of $(\overline{\phi_s}, \overline{i_s})$ |

# References


[1] Q.T. An, L. Sun and L.Z. Sun, "Current Residual Vector Based Open Switch Fault Diagnosis of inverters in PMSM Drive Systems". *IEEE Trans. On Power Electron, vol. 30, pp. 2814-2827,* May. 2015.

[2] Thomas Finken, Matthias Felden and Kay Hameyer, "Comparison and design of different electrical machine types regarding their applicability in hybrid electrical vehicules". *Proceedings of the 2008 International Conference on Electrical Machines,* pp. 1-5, 2008.

[3] Asma Boulmane, Youssef Zidani. Mohammed Chennani and Driss Belkhayat. "Design of Robust Adaptive Observer against Measurement Noise for Sensorless Vector Control of Induction Motor Drives". *Journal of Electrical and Computer Engineering, Hindawi,* 2020.

[4] Taichi Nishio, Yamauchi Ryosuke, Kondo Masahiko, Kan Akatsu, "A Method of Torque Ripple Reduction by Using Harmonic Current Injection in PMSM". *IEEE 4th International Future Energy Electronics Conference (IFEEC),* 2019.

[5] A. F. Shcvchenko and L. G. Shevchenko, "The Problem of Electromagnetic Torque Ripples in Synchronous Motor". *XIV International Scientific-Technical Conference on Actual Problems of Electronics Instrument Engineering (APEIE),* pp. 406-409, 2018.

[6] Mauricio Cuevas, "Méthodes non-invasives de diagnostic de défauts et d'analyse". Ph.D thesis, 2017.

[7] A. CEBAN, "METHODE GLOBALE DE DIAGNOSTIC DES MACHINES". Ph.D thesis, 2012.

[8] E. Bahri, R. Pusca, R. Romary, D. Belkhayat, "Minimization of torque ripple caused by a stator winding dissymmetry in a surface permanent magnet synchronous machine". *International Conference on Electrical Machines (ICEM),* pp. 221-226, 2014.

[9] E. S. Xavier Kestelyn, "A Vectorial Approach for Generation of Optimal Current References for Multiphase Permanent-Magnet Synchronous Machines in Real Time". *IEEE Transactions on Industrial Electronics,* vol. 58, pp. 5057 - 5065, 2011.

[10] A.H. Abosh, Z.Q. Zhu, "Current Control of permanent magnet synchronous machine with asymmetric phases". *7th IET International Conference on Power Electronics, Machines and Drives* , 2014.

[11] Elmehdi Bahri, Driss Belkhayat, Remus Pusca, Raphael Romary, "Torque ripple control in faulty surface permanent magnet synchronous motor". *International Conference on Applied and Theoretical Electricity (ICATE),* 2016.

[12] A. a. A.Zuckerberger, "Space-phasor model of a three-phase induction motor with a view to digital simulation". *Electric PowerSystems Research,* vol. 12, pp. 157-165, 1987.

[13] Mauricio Cuevas, Raphaël Romary, Jean-Philippe Lecointe, Thierry Jacq, "Non-Invasive Detection of Rotor Short-Circuit Fault in Synchronous Machines by Analysis of Stray Magnetic Field and Frame Vibrations". *IEEE Transactions on Magnetics,* vol. 52, 2016.

[14] Andrian Ceban, Remus Pusca, Raphaël Romary, "Study of Rotor Faults in Induction Motors Using External Magnetic Field Analysis". *IEEE Transactions on Industrial Electronics,* vol. 59, pp. 2082 - 2093, 2012.